Proceedings of the Jangjeon Mathematical Society
24 (2021), No. 4, pp. 457 - 479
www.jangjeon.or.kr
http://dx.doi.org/10.17777/pjms2021.24.4.457

# INTRINSIC STRUCTURE AND HIGH SPIN POSITIVE PARITY STATES IN DOUBLY EVEN SE ISOTOPES

RAJAT GUPTA, RIDHAM BAKSHI, SURAM SINGH, AND ARUN BHARTI

Abstract. A systematic study of nuclear structure properties of proton rich even-even positive parity $^{80,82,84}$Se isotopes have been studied within two-body self-consistent quantum mechanical framework known as Projected Shell Model (PSM)which incorporates quadrupole-quadrupole, monopole and quadrupole pairing interactions. The description of band structures of even-even $^{80,82,84}$Se nuclei based on the band diagrams indicates the presence of multi-quasi-particle structure which provides us a unified understanding of ever accumulating high spin structure of these nuclei. The back-bending in moment of inertia, yrast spectra and g-factor have also been obtained and are also compared with the available experimental data.

Keywords and phrases. Projected Shell Model (PSM); yrast spectra; back bending; band diagram; g-factor.

---

[1]Date of Paper Submission: 18 Sept. 2019

Author, Rajat Gupta acknowledges the financial support under NET-JRF from University Grants Commission (UGC) under Id No.: 201610140311.One of the co-author, Ridham Bakshi, also acknowledges the financial support from The Department of Science and Technology, Government of India, INSPIRE Fellowship under sanction no. DST/INSPIRE Fellowship/2018/IF180368. The authors of the present paper also express their gratitude to Prof. J. A. Sheikh and Dr. G. H. Bhat for their suggestions.

## 1. Introduction

Nuclei in the mass-80 region had been on the line of description since the past many years because of the occurance of a wide variety of nuclear structure phenomena [1, 2, 3, 4] that are unique to this mass region and also the strong variation of these phenomena with both particle number and spin. Experiments made in the past [5, 6] have shown that this region contains some of the most deformed nuclei of the periodic table. The microscopic structure of the nuclei in the A$\approx$80 mass region is primarily determined by the $g_{9/2}$, $p_{1/2}$, $f_{5/2}$, and $p_{3/2}$ orbitals. The shell-structure effects in this mass region give rise to a strong shape variation. In comparison to the rare-earth region where the change in nuclear structure properties is quite smooth with respect to particle number, the proton-rich mass-80 nuclei shows considerable variation in their nuclear structure when going from one nucleus to another which is due to the fact that the available shell model configuration space in the mass-80 region is much smaller than in the rare-earth region.

Among the various nuclei present in the medium to heavy mass region in the nuclear chart, the nuclear deformation has been observed for both neutron-rich as well as neutron-deficient isotopes present in the mass region A$\approx$80 [1] and experimentally, it has been observed that nuclei like Kr, Sr and Zr [7, 8, 9, 10] lying in the mass-80 region have deformed mass distribution and behave like well-deformed rotors. In the past few years, low-lying energy states in several isotopes have been measured for the first time or re-measured with higher precision in the A$\approx$80 mass region [11, 12, 13, 14]. In the past years, Se isotopes have been precisely studied, experimentally as well as theoretically, by various research groups[15, 16, 17, 18, 19, 20, 21, 22, 23, 24]. In the recent past, the high spin excitations and level scheme of Se isotopes have been studied experimentally upto spin $10^+$[15, 23].

The present piece of work uses a self-consistent quantum mechanical approach i.e. Projected Shell Model (PSM) [25] which uses deformed Nilsson basis to explain the deformation characteristics of some proton rich doubly even nuclei ($^{80,82,84}$Se) lying in the A≈80 region. In this work, the level scheme for $^{80,82,84}$Se has been further extended to higher values of spin i.e. upto spin $20^+$ to investigate the high-spin characteristics of the nuclei under study. Also, the deformed nuclear structure is explained in terms of their deformation systematics as well as nuclear structure properities like yrast energy states, band diagrams, backbending in momemt of inertia, g-factors and BE2 values. The present work is divided into different sections as follows.A brief outline of the model used is given in section 2. In section 3, theoretical analysis of PSM results and their comparison with experimental counterparts is presented. At the last, summary and conclusion is given in section 4.

## 2. Methodology

2.1. **Outline of PSM-An Quantum Mechanical Approach.** The shell model is the most fundamental way of describing many body nucleon system quantum mechanically. But it suffers from a serious disadvantage that, it can be applied only for spherical nuclei and most of the nuclei present in the nuclear chart are deformed, except those lying in the vicinity of magic numbers. Therefore it is not possible to treat such nuclei within the framework of spherical shell model. Also using such a shell model to study arbitrarily heavy deformed nuclei is impossible because of the requirement of huge dimensionality of the configuration space and related problems. Therefore, a modified version of shell model was developed known as Projected Shell Model which is well applicable to deformed nuclei also. The generalization of the phenomenological shell model to deformed shapes was first given by S.G Nilsson [26] by modifying shell model Hamiltonian to explain the microscopic structures of the deformed nuclei. Elliott [27, 28] was the first to point out the advantage of deformed (intrinsic) many-body basis and developed the SU(3) shell model for s-d shell nuclei. The PSM can be considered to be a natural extension of the Elliott SU(3) shell model to heavier systems, which makes shell-model calculation for heavy, deformed nuclei feasible.

Projected Shell Model (PSM) technique is the generalization of the shell model, for heavy deformed nuclei. The Projected Shell Model has been designed to meet the quality of measurements by using modern techniques and has an advantage that the truncation of the configuration space can be done very effectively. Projected Shell Model uses more physical states (e.g. solutions of a deformed mean field) and angular momentum projection technique [29, 30, 31, 32, 33] to build shell model basis and is a bridge between shell model and mean field method. The PSM is built over a deformed mean field, which incorporates pairing effects through a Bogolyubov transformation to quasiparticle states. Both the Nilsson deformation parameter and the pairing constants are taken from systematics. The projected Bardeen-Cooper-Schrieffer (BCS) vacuum gives the unperturbed ground state band in even even nuclei, while unperturbed excited bands are obtained by projecting the multi-quasiparticle states. The multi-quasiparticle states are those with two proton and two neutron quasiparticle excitations (for even even nuclei), with proton-neutron quasiparticle pairs (for odd-odd nuclei), or with one and three quasiparticle states (for odd mass nuclei). The most striking aspect of this quantum mechanical model is its ability to describe the inner details of the high-spin spectroscopy data with simple physical interpretations.

The chosen multi-qp subspace for the present study of even-even Se isotopes is given below

**Doubly-even nucleus:**

$$|0\rangle,\ a^{\dagger}_{\nu1}a^{\dagger}_{\nu2}|0\rangle,\ a^{\dagger}_{\pi1}a^{\dagger}_{\pi2}|0\rangle,\ a^{\dagger}_{\nu1}a^{\dagger}_{\nu2}a^{\dagger}_{\pi1}a^{\dagger}_{\pi2}|0\rangle$$

Where $\nu^{,s}(\pi^{,s})$ denote the neutron(proton) Nilsson quantum numbers which run over properly selected (low-lying) quasiparticle states. The Hamiltonian used in this calculational framework consists of a sum of schematic (Quadrupole-Quadrupole + Monopole pairing + Quadrupole pairing) forces which represent different kinds of characteristic correlations between the active nucleons. The total Hamiltonian is of the form

$$\hat{H} = \hat{H}_0 - \frac{1}{2}\chi \sum_{\mu} \hat{Q}^{\dagger}_{\mu}\hat{Q}_{\mu} - G_M \hat{P}^{\dagger}\hat{P} - G_Q \sum_{\mu} P^{\dagger}_{\mu}P_{\mu} \tag{1}$$

where $\hat{H}_0$ represents the spherical single particle Shell Model Hamiltonian involving spin-orbit interactions while the second, third and fourth terms represent the quadrupole-quadrupole, monopole and quadrupole pairing interactions respectively. denotes the strength of quadrupole-quadrupole two-body interaction and is adjusted with the quadrupole deformation parameter, $\epsilon_2$.

The monopole pairing strength $G_M$ is given by

$$G_M = \left\{ G_1 \mp G_2 \frac{N-Z}{A} \right\} \frac{1}{A} (MeV), \tag{2}$$

with "+" for protons and "-" for neutrons. $G_1$ and $G_2$ are two adjustable parameters. For the present set of PSM calculations, three major shells (N = 2, 3, 4) for both protons and neutrons have been chosen.

Table 1. and Table 2., display the various sets of input interaction parameters used for performing nuclear structure calculations on Selenium isotopes. The first set of input parameters used in the PSM calculations are the Nilsson parameters, $\kappa$ and $\mu$ and are taken in such a manner that they reproduce the best fit of available experimental data. The second set of input parameters used are the empirical deformations, quadrupole deformation ($\epsilon_2$) and Hexadecupole deformation ($\epsilon_4$). The strength of the quadrupole force, $G_Q$, is assumed to be proportional to $G_M$ and its value and the pairing interaction strengths selected for the present set of calculations for all the isotopes under study are given in the Table 1. Further the values of quadrupole and Hexadecupole deformation parameters ($\epsilon_2$ and $\epsilon_4$) used in the present work are shown in the Table 2.

## 3. Analysis of Results

The detailed description of various results obtained by performing the Projected Shell Model (PSM) calculations for the study of even-even $^{80,82,84}$Se isotopes have been given in this section. Interesting nuclear structure properties such as yrast spectra, band structure, back-bending in moment of inertia and g-factor have been obtained. The results of PSM calculations are then compared with the available experimental to bring out some important underlying physics.

3.1. **Yrast Spectra.** Yrast band is the lowest energy band comprising of lowest energy states for a given angular momentum. In Fig.1 the PSM results on yrast energy states for even-even $^{80,82,84}$Se isotopes are plotted against the spin and are compared with the experimentally available data [34] and also with the results obtained by JUN45 and jj44b interactions [15, 16]. The experimental data for yrast energy levels for even-even $^{80,82,84}$Se isotopes is available only upto spin $I = 10\hbar$ while PSM calculation are able to predict the results to higher values of spin i.e. upto last calculated spin $20\hbar$.

Thus, it is found that the experimental energy states are very well replicated by the projected shell model calculations for $^{80,82,84}$Se isotopes. Besides this, the PSM calculations are able to successfully reproduced the band-head spins for the isotopes under study.

3.2. **Projected quasi-particle configuration and configuration mixing.** A band diagram is an ensemble of projected quasi-particle configurations all plotted together. A band diagram is a very important tool for analyzing the PSM results and plays a crucial role for the interpretation of the yrast states obtained as a result of diagonalisation within the chosen deformed basis states. Due to the presence of energy differences of various bands, there occurs crossing of bands at certain value of spin where some prominent phenomena (like back-bending in moment of inertia, variation in g-factor and many more) may take place, and therefore plays a central role in the interpretation of the numerical results. The rotational frequency of the yrast band will decrease suddenly at a band crossing point since, in the band diagram, the slope of the crossing band is smaller than that of the crossed band, otherwise no crossing can take place. This indicates that the rotational frequency suddenly becomes smaller when there occurs a band crossing. In present case, the configuration space is built by many quasi-particles (qp) bands, but only a few most important lowest ones have been plotted to illustrate the important physics. Moreover, each band has been marked with the corresponding qp-configuration.

From Fig.2(a), for $^{80}$Se one observes that the yrast spectra upto spin $4^+$ coincides with the g-band arising from 0-qp intrinsic state. At spin $4^+$, the g-band is crossed by 2-qp neutron band having configuration $2\nu g_{9/2}$[5/2,-7/2], K = -1, which contributes to yrast upto spin $12^+$. The yrast states from spin $12^+$ to the last calculated spin have complex structure, as they arise from the superposition of 2-qp proton bands having configuration $2\pi f_{5/2}$[1/2, -3/2], K= 2 and 4-qp band having configuration $2\nu g_{9/2}$[5/2, -7/2] + $2\pi f_{5/2}$[1/2, -3/2], K= -2, crosses the 2-qp neutron and proton bands and becomes yrast from spin $12^+$ upto the last calculated spin $20^+$.

For $^{82}$Se (Fig. 2(b)), it is evident that the yrast spectrum upto spin $8^+$ coincides with the g-band and at spin $8^+$ the g-band is crossed by 2-qp proton band having configuration $2\pi f_{5/2}$[1/2, -3/2], K = -1 and becomes yrast upto spin $14^+$. At spin $14^+$, the above mentioned 2-qp proton band is crossed by the three 4-qp bands having configuration $2\nu g_{9/2}$[-7/2,1/2] + $2\pi f_{5/2}$[1/2,1/2], K = -3, $2\nu g_{9/2}$[-7/2,1/2]+ $2\pi f_{5/2}$[1/2,-3/2], K = -4, $2\nu g_{9/2}$[-7/2,1/2]+ $2\pi f_{5/2}$ [1/2,-3/2], K = -2 resulting in complex structure and superposition of these bands contribute to the yrast upto the last calculated spin $20^+$.

For $^{84}$Se (Fig. 2(c)), one can notice that the yrast states upto $5^+$ arise from g-band. At spin $5^+$ the 2-qp neutron band having configuration $2\nu g_{9/2}$[1/2,1/2], K = 1 crosses the g-band and contributes to the yrast upto spin $10^+$. From spin $10^+$ upto calculated spin $16^+$ the yrast state is mainly contributed by the superposition of two 4-qp bands having configuration $2\nu g_{9/2}$[1/2,1/2] + $2\pi f_{5/2}$[1/2,-3/2], K = -1 and $2\nu g_{9/2}$[1/2,1/2] + $2\pi f_{9/2}$[1/2,-3/2], K = 0.

From the overall analysis of the band diagram for $^{80,82,84}$Se isotopes, one may conclude that at lower values of spin, the 2-qp bands are the dominating ones, but at higher spin side, the 4-qp (two quasiproton plus two quasineutrons) bands contributes to the yrast formation. This indicates the presence of multi-quasiparticle structure of $^{80,82,84}$Se isotopes. Therefore, PSM calculations predicts that these nuclei might have the composite structure at the higher excited states.

3.3. **Back-Bending in moment of inertia.** When there appears a discontinuity in the rotational levels of some deformed nuclei at the time of variation of moment of inertia with the square of the rotational frequency, there occurs a backbend and the phenomenon is known as back-bending. Backbending is a prominent phenomenon and generally occurs at those values of spins where the band crossing takes place. It can be represented as a plot between twice the kinetic moment of inertia and square of rotational frequency ($\hbar^2\omega^2$), calculated using the formulae [35]

$$2\Im^{(1)} = \frac{(2I-1)}{\omega}(\hbar^2 MeV^{-1}) \tag{3}$$

$$\hbar\omega = \frac{E_\gamma}{\sqrt{(I+1)(I+2)-K^2} - \sqrt{(I-1)I-K^2}} \tag{4}$$

Fig.3 represents the backbending plots for even-even $^{80,82,84}$Se isotopes where PSM and experimental results are plotted for the sake of comparison. It can be seen that, in $^{80}$Se (see Fig.3(a)), the experimental results exhibits backbending at spin $6^+$, and the theoretical PSM results also reproduce the backbending at the same spin i.e. at $6^+$. Moreover, the theoretical calculations are also able to predict backbending at higher values of spin i.e. at $12^+$ and $18^+$, but the corresponding experimental data is not available to make the comparison at higher spins. For $^{82}$Se (see Fig.3(b)), the backbending is experimentally observed at $6^+$. The theoretical results also show that the backbending appears at spin $6^+$. Theoretically, backbending has also been observed at higher spins also, at $12^+$ and $14^+$, but experimental data is not available at higher spins. In case of $^{84}$Se (see Fig.3(c)) experimentally, one observes backbending at spin $2^+$ and the theoretical results predicts this trend at a later value of spin $6^+$, but at almost same rotational frequency.

Thus, it can be concluded from the present calculations that backbending in moment of inertia for $^{80,82,84}$Se occurs at almost same spin as observed experimentally in most of the nuclei under study, this supports the accuracy of the calculated PSM results. However, the comparison cannot be made at higher spins due to the non-availability of the experimental data.

3.4. **Deformation Systematics of $^{80,82,84}$Se nuclei.** It is well known from the Grodzin's rule [36] that higher the value of E($2_1^+$),lesser is the deformation in a nucleus or in other words, one can say that the energy of first excited state i.e.E($2_1^+$) of any nucleus is inversely proportional to its quadrupole moment. In order to see this kind of systematics in the present work, the PSM calculations on $^{80,82,84}$Se are performed to evaluate the energy of first excited state E($2_1^+$) in these nuclei. For performing the present set of calculations, a set of values of quadrupole deformation are used as an input parameter in PSM calculations. Now, the energy of E($2_1^+$)state obtained in the present PSM calculations and the various values of quadrupole deformation ($\epsilon_2$) used as an input parameter for $^{80,82,84}$Se are presented in Table 3.

It is very much clear from the data presented in the Table 3. that the Grodzin's rule is satisfied by the present PSM calculations. As can be seen from the table, the value of E($2_1^+$) is increasing as one goes from $^{80}$Se to $^{84}$Se nucleus, whereas the value of $\epsilon_2$ decreasing as one goes from $^{80}$Se to $^{84}$Se nucleus. For example, the E($2_1^+$) value increases from 0.6981 MeV for $^{80}$Se to 1.5356 MeV for $^{84}$Se and the value of $\epsilon_2$ is decreasing from 0.210 units for $^{80}$Se to 0.185 units for $^{84}$Se, indicating the opposite behaviour of the quadrupole deformation with the systematics of E($2_1^+$).

Thus, from the above discussion, it is evident that the present PSM calculations performed for $^{80,82,84}$Se nuclei are in good agreement with the expected trend as suggested by the Gordinz's rule. Moreover, the calculated PSM values of E($2_1^+$) are in quite good agreement with their experimental counterparts.

3.5. **Electric quadrupole [B(E2↓)] transition probability.** Reduced transition probability B(E2↓) is a measure of collectivity for a nucleus. The reduced electric quadrupole transition probability is one of the important nuclear structure properties which provides information about the nuclear structure. By comparing experimentally determined B(E2↓) values with those obtained by performing Projected Shell Model calculations, conclusions can be drawn about the nature of the excitations and transitions.

The values of reduced electric quadrupole transition probability have been calculated using the formula [37] as given below

(5)
$$B(E2) = e^2 Q_0^2 \frac{15}{32\pi} \frac{(I-1-K)(I-1+K)(I-K)(I+K)}{(I-1)(2I-1)I(2I+1)}$$

Here, $e^2Q_0^2 = [e_\nu Q_\nu + e_\pi Q_\pi]^2$, where $Q_\nu(Q_\pi)$ are the intrinsic quadrupole moments of the valence neutrons (protons) as predicted by PSM wavefunction and $e_\nu(e_\pi)$ are the effective charges of the neutrons (protons), respectively.

Table 4. shows the theoretical results of reduced electric transition probabilities B(E2) values and are compared with experimental results and the results obtained from various other interactions i.e. JUN45 and jj44b interactions [15]. The experimental and theoretically calculated PSM results are found to be in good agreement.

3.6. **STUDY OF g-FACTOR.** Gyro-magnetic ratios provide insights into many nuclear structure questions since they are sensitive to contributions from both collective and single-particle degrees of freedom. . It provides important information about the microscopic structures of the yrast states and is defined as as given in ref.[38]

The g-factors of $2_1^+$and $4_1^+$states for $^{80,82,84}$Se nuclei are displayed in Fig. 4 in terms of the individual contribution from protons ($g_\pi$) and neutrons ($g_\nu$), the sum of which is the total g-factor ($g_{total}$), and are compared with the available experimental data. It has been observed (see Fig. 4) that the proton and neutron contribution shows almost opposite trends. Also the neutron contribution to the g-factor is very small, so the variations in the g-factor are almost due to the proton contribution only. The values of the g-factors are plotted against the spin and it has been found that the g-factors show an increase or decrease around that value of spin for which there occurs band crossing which can be verified from Fig.2. The experimental trend of g-factors of $^{80,82,84}$Se has been quite satisfactorily.

From Fig.4(a) for $^{80}$Se, it is observed that the theoretical values of g-factor show a small increase around spin $4^+$ followed by a sharp increase around spin $12^+$. Now looking at the trend of band diagram in $^{80}$Se(Fig.2(a)), one observed that the band crossing occurs at spin $4^+$, where a 2-qp neutron band crosses the g-band and also at spin $12^+$, where the 4-qp band crosses the 2-qp band respectively.

In Fig.4(b), there appears small increase in the value of the g-factor at spin $6^+$ which results from the crossing of the g-band by 2-qp proton band (as seen from Fig.2(b)) and also there is again small increase in g-factor at spin $14^+$, this is due to the crossing of the 2-qp proton band by 4-qp bands arising from $g_{9/2}$ orbitals. From Fig.4(c), it is observed that there is a sharp decrease in g-factor at spin $4^+$ and corresponding crossing of g-band by 2-qp neutron band is also seen from Fig.2(c) at the same spin. Again at some higher spin around $12^+$, there is small rise in the g-factor values and around same spin a 2-qp neutron band is crossed by two 4-qp bands arising from $g_{9/2}$ orbitals.

Thus, from above discussion it is found that the value of g-factors increases of decreases at the same spin value at which there is band crossing in $^{80,82,84}$Se isotopes, thus gives the evidence of occurrence of the structural changes at those spin values.

## 4. SUMMARY

From the comparison of data obtained from PSM approach with experimentally available data, one can conclude the nuclear structure phenemenon for positive-parity states of $^{80,82,84}$Se isotopes are well explained in terms of various nuclear structure properities such as yrast energy states, back-bending in moment of inertia, deformation systematics, band diagrams etc. The PSM results are in very good agreement with the experimental counterparts. Moreover, the band-heads have been also predicted correctly.

## 5. Tables and Figures

Table 1. Values of input parameters used in the present PSM calculations of even-even Se isotopes for positive parity.

| Set of Parameters | Values |
|---|---|
| $G_1$ | 22.25 |
| $G_2$ | 14.20 |
| $G_Q/G_M$ | 0.18 |

TABLE 2. Values of deformation parameters i.e. $\epsilon_2$ and $\epsilon_4$, used in present PSM calculations

| Isotopes | $\epsilon_2$ | $\epsilon_4$ |
|---|---|---|
| $^{80}$Se | 0.210 | 0.000 |
| $^{82}$Se | 0.240 | 0.000 |
| $^{84}$Se | 0.185 | 0.000 |

TABLE 3. Systematics of calculated first excited energies $E(2_1^+)$(in MeV) for $^{80,82,84}$Se isotopes.

| Isotopes | $E(2_1^+)$ (PSM) | $E(2_1^+)$ (Expt.) | $\epsilon_2$ |
|---|---|---|---|
| $^{80}$Se | 0.6981 | 0.6662 | 0.210 |
| $^{82}$Se | 0.6908 | 0.6457 | 0.240 |
| $^{84}$Se | 1.5356 | 1.4545 | 0.185 |

Table 4. B(E2) reduced transition strength in $e^2\ b^2$, Experimental values were taken from the NNDC database.

| $BE2(2_1{}^+ \to 0_1{}^+)$ | $^{80}Se$ | $^{82}Se$ | $^{84}Se$ |
|---|---|---|---|
| PSM | 0.05402 | 0.0676 | 0.0487 |
| Experimental | 0.05287 | 0.03648 | N/A |
| JUN45 | 0.03611 | 0.03032 | 0.0145 |
| jj44b | 0.04125 | 0.03349 | 0.0182 |
| $BE2(4_1{}^+ \to 2_1{}^+)$ | $^{80}Se$ | $^{82}Se$ | $^{84}Se$ |
| PSM | 0.0827 | 0.1035 | 0.0786 |
| Experimental | 0.07581 | 0.04085 | N/A |
| JUN45 | 0.04675 | 0.04282 | 0.0043 |
| jj44b | 0.05604 | 0.04543 | 0.0000 |
| $BE2(6_1{}^+ \to 4_1{}^+)$ | $^{80}Se$ | $^{82}Se$ | $^{84}Se$ |
| PSM | 0.0983 | 0.1242 | 0.0946 |
| Experimental | N/A | N/A | N/A |
| JUN45 | 0.0367 | 0.0337 | 0.0002 |
| jj44b | 0.0479 | 0.0393 | 0.0071 |
| $BE2(8_1{}^+ \to 6_1{}^+)$ | $^{80}Se$ | $^{82}Se$ | $^{84}Se$ |
| PSM | 0.1111 | 0.1411 | 0.1087 |
| Experimental | N/A | 0.00122 | N/A |
| JUN45 | 0.0163 | 0.00083 | 0.0000 |
| jj44b | 0.0028 | 0.00068 | 0.0000 |

(6)

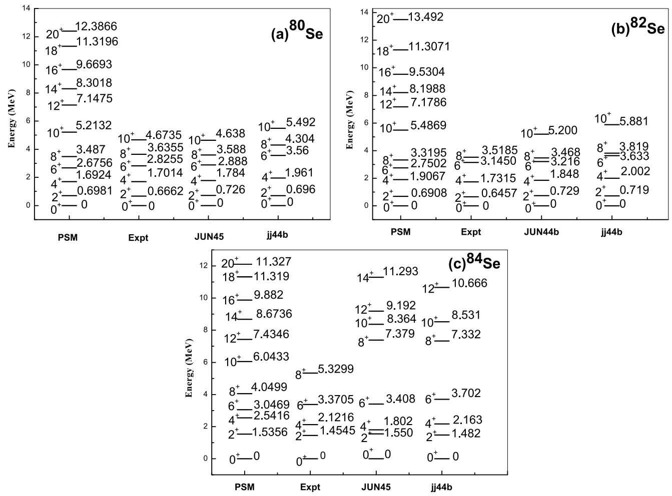


FIGURE 1. Comparison of yrast energy states (Th.) with experimental data and with the results of JUN45 and jj44b interaction terms for (a)$^{80}$Se (b)$^{82}$Se and (c)$^{84}$Se

(7)

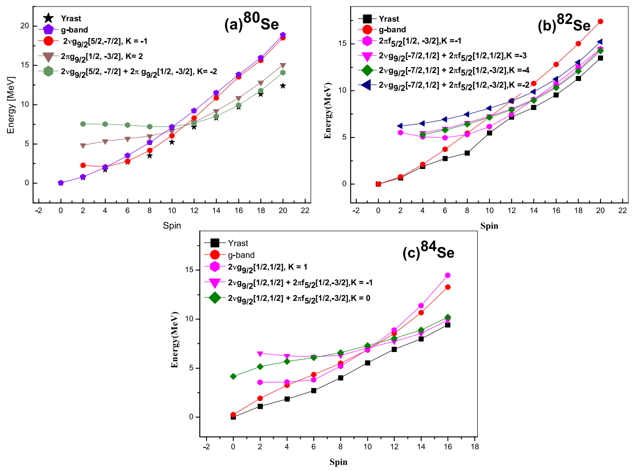


FIGURE 2. Band diagrams for (a) $^{80}$Se (b) $^{82}$Se (c) $^{84}$Se isotopes

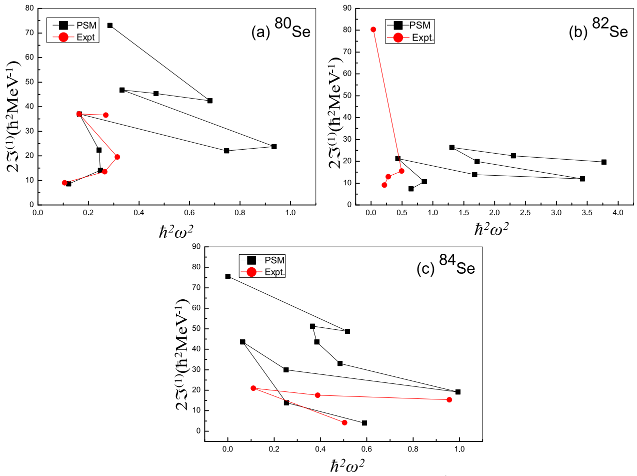


FIGURE 3. Moment of inertia ($\Im^1$) plotted against angular frequency squared ($\hbar^2\omega^2$) and compared with experimental data for (a)$^{80}$Se (b)$^{82}$Se (c)$^{84}$Se isotopes

(9)

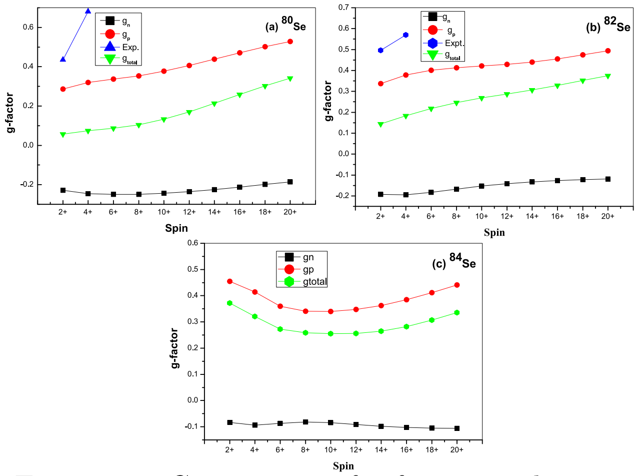


FIGURE 4. Comparison of g-factor results (Th.) with experimental data for $^{80,82,84}$Se isotopes.

## References


[1] Jürgen Eberth *et al., Nuclear Structure of the Zirconium Region*, Springer-Verlag 71 (1988), 1502.

[2] H. G. Price *et al., Observation of Rigid Nuclear Rotation*, Phys. Rev. Lett. 51 (1983), 1842.

[3] E.F. Moore *et al., Shape coexistence effects and quasiparticle alignment in* $^{81}$Sr, Phys. Rev. C 38 (1988), 696.

[4] W. Nazarewicz *et al., Microscopic study of the high-spin behaviour in selected A 80 nuclei*, Nucl. Phys. A 435 (1985), 397.

[5] C. J. Lister *et al., Extreme Prolate Deformation in Light Strontium Isotopes*, Phys. Rev. Lett. 49 (1982), 308.

[6] R.B. Piercey *et al., Evidence for Deformed Ground States in Light Kr Isotopes*, Phys. Rev. Lett. 47 (1981), 1514.

[7] C.J. Lister *et al., Gamma radiation from the N=Z nucleus* $^{80}_{40}\mathrm{Zr}_{40}$, Phys. Rev. Lett. 59 (1987), 1270.

[8] D.F. Winchell *et al.,Structure of normally deformed states in* $^{80}Sr$, Phys. Rev. C 61 (2000), 044322.

[9] S.M. Fischer *et al., Alignment Delays in the* $N = Z$ *Nuclei* $^{72}Kr$, $^{76}Sr$, *and* $^{80}Zr$, Phys. Rev. Lett. 87 (2001), 132501.

[10] E. Bouchez *et al., New Shape Isomer in the Self-Conjugate Nucleus* $^{72}$Kr, Phys. Rev. Lett. 90 (2003), 082502.

[11] T. J. Mertzimekis *et al., Systematics of first* $2^+$ *state g factors around mass 80*, Phys. Rev. C 68 (2003), 054304.

[12] O. Kenn *et al., Measurements of g factors and lifetimes of low-lying states in* $^{62-70}$Zn *and their shell model implication*, Phys. Rev. C 65 (2002), 034308.

[13] K.H. Speidel *et al., Shell closure effects in the stable* $^{74-82}Se$ *isotopes from magnetic moment measurements using projectile excitation and the transient field technique*, Phys. Rev. C 57 (1998), 2181.

[14] T.J. Mertzimekis *et al., First measurements of the g factors in the even Kr isotopes*, Phys. Rev. C 64 (2001), 024314.

[15] J. Litzinger *et al., Transition probabilities in neutron-rich* $^{80,82}$Se *and the role of the* $\nu g_{9/2}$ *orbital*, Phys. Rev. C 97 (2018), 044323.

[16] P.C. Srivastava,*et al., Comparison of shell model results for even-even Se isotopes*, Phys. Scr. 88 (2013), 045201.

[17] A. Makishima *et al.,* $(\nu g_{9/2}^{-2})_{8^+}$ *isomers* in$^{82}\mathrm{Se}_{48}$ *and* $^{80}\mathrm{Ge}_{48}$ *populated by deep-inelastic collisions*, Phys. Rev. C 59 (1999), R2331.

[18] G. A. Jones *et al., Yrast studies of* $^{80,82}$Se *using deep-inelastic reactions*, Phys. Rev. C 76 (2007), 054317.

[19] Nurettin Türkan *et al., IBM-2 calculations of some even-even selenium nuclei* Cent. Eur. Journal of Physics 4 (2006), 124.

[20] K. P. Lieb and J. J. Kolata *Ground-state band in* $^{72}$Se, Phys. Rev. C 15 (1977), 939.

[21] F. S. Radhi *et al., An IBM description of* $^{76}$*Se and neighbouring Se-isotopes*, Zeitschrift für Physik A Hadrons and Nuclei 356 (1996), 145.

[22] T. Hayakawa *et al., Projectile Coulomb excitation of* $^{78}$Se, Phys. Rev. C 67 (2003), 064310.

[23] M.G. Porquet *et al., High-spin excitations of* $^{81,82,83,85}$*Se : Competing single-particle and collective structures around* $N = 50$, Eur. Phys. J 39 (2009), 295.

[24] E. F. Jones *et al., Identification of* $^{88}$Se *and new levels in* $^{84,86}$Se, Phys. Rev. C 73 (2006), 017301.

[25] Yang Sun *et al., Projection techniques to approach the nuclear many-body problem*, Physica Scripta 91 (2016), 4.

[26] S.G. Nilsson *Nuclear Structure Vol.II: Nuclear deformations*, Dan. Mat. Fsy. Medd. 29 (1995) 16.

[27] J. P. Elliott *Collective Motion in the Nuclear Shell Model. I.Classification Schemes for States of Mixed Configurations*, Proc. R. Soc. Lond. A 245 (1958), 245.

[28] J. P. Elliott and M. Harvey *Collective Motion in the Nuclear Shell Model. III. The Calculation of Spectra*, Proc. R. Soc. Lond. A 272 (1963), 557.

[29] K. Hara and S. Iwasaki *et al., On the quantum number projection: (I). General theory*, Nucl. Phys. A 332 (1979), 61.

[30] K. Hara and S. Iwasaki *et al., On the quantum number projection: (III). Simultaneous J- and N-projection*, Nucl. Phys. A 348 (1980), 200.

[31] S. Iwasaki and K. Hara *Treatment of the Band Crossing by Means of the Angular Momentum Projection Method* , Prog. Theor.Phys. 68 (1982), 1782.

[32] K. Hara and S. Iwasaki *An analysis of odd-mass rare-earth nuclei using angular momentum projection*, Nucl. Phys. A 430 (1984), 175.

[33] P. Ring, P. Schuck *The Nuclear Many-Body Problem*,Springer-Verlag, New York, (1980).

[34] Balraj Singh *Nuclear Data Sheets for A = 80*, Nuclear Data Sheets 105 (2005), 223.

[35] Ibáñez-Sandoval,*et al., Projected shell model study of yrast states of neutron-deficient odd-mass Pr nuclei*, Phys. Rev. C 83 (2011), 034308.

[36] L. Grodzins *The uniform behaviour of electric quadrupole transition probabilities from first 2sup+ states in even-even nuclei*, Phys. Lett. 2 (1962).

[37] A.Bohr, B.R. Mottelson *Nuclear Structure Vol.II: Nuclear deformations*, World Scientific (1999).

[38] Y. Sun and J.L. Egido, *Angular-momentum-projected description of the yrast line of dysprosium isotopes*, Nucl. Phys. A 580 (1994),1.

Department of Physics, University of Jammu,, Jammu - 180006, India

*Email address*: rajatgupta710@gmail.com

Department of Physics, University of Jammu,, Jammu - 180006, India

*Email address*: ridham4bakshi@gmail.com

Department of Physics, University of Jammu,, Jammu - 180006, India

*Email address*: suramsingh@gmail.com

Department of Physics, University of Jammu,, Jammu - 180006, India

*Email address*: arunbharti_2003@yahoo.co.in